

X-ray absorption of N₂ accompanied by infrared-induced transitions between the ungerade and gerade core levels

This content has been downloaded from IOPscience. Please scroll down to see the full text.

2008 J. Phys. B: At. Mol. Opt. Phys. 41 145601

(<http://iopscience.iop.org/0953-4075/41/14/145601>)

View [the table of contents for this issue](#), or go to the [journal homepage](#) for more

Download details:

IP Address: 159.178.22.27

This content was downloaded on 01/10/2015 at 20:07

Please note that [terms and conditions apply](#).

X-ray absorption of N₂ accompanied by infrared-induced transitions between the ungerade and gerade core levels

Yasen Velkov¹, Ji-Cai Liu^{1,2}, Chuan-Kui Wang^{1,2}
and Faris Gel'mukhanov¹

¹ Department of Theoretical Chemistry, School of Biotechnology, Royal Institute of Technology, S-10691 Stockholm, Sweden

² College of Physics and Electronics, Shandong Normal University, 250014 Jinan, People's Republic of China

E-mail: yasve@theochem.kth.se

Received 17 April 2008, in final form 2 June 2008

Published 30 June 2008

Online at stacks.iop.org/JPhysB/41/145601

Abstract

We study a two-colour pump–probe scheme of x-ray absorption accompanied by core-hole hopping in the field of a strong IR laser. The process is exemplified for fixed-in-space and randomly oriented homonuclear diatomic molecules N₂ near the $1\sigma_u \rightarrow 1\pi_g$ x-ray absorption transition. The laser field mixes the core holes of opposite parities and causes Rabi splitting of the core-excited states. The IR field results in spectral broadening and shifts of the x-ray resonances as well as decrease of x-ray photoabsorption. The Stark broadening of the x-ray absorption spectrum depends on the orientation of the molecule and the angle between the polarization vectors of the x-ray and IR fields. The spectral changes caused by the IR field are weaker for randomly oriented molecules in comparison with fixed-in-space molecules.

1. Introduction

X-ray absorption (XA) spectroscopy of randomly oriented [1] and fixed-in-space molecules [2] is a powerful and widely used investigation technique with numerous scientific applications. By measuring the absorption of x-ray photons as a function of the incident x-ray energy, one can obtain element-specific structural information about density of states, nature of chemical bonds, surrounding environment, molecular orientation, etc [3]. Owing to the development of the synchrotron-radiation and laser sources, the XA spectroscopy can be utilized further to provide unique and valuable information on electron dynamics that is often difficult to access by other experimental means. Indeed, the combination of brilliant x-ray sources and harmonic generation with strong infrared (IR) or visible laser light gives a new tool in the x-ray spectroscopy—namely, the x-ray pump–probe spectroscopy [3–6]. In the typical x-ray pump–probe schemes, the laser field plays the role of a pump acting on the ground state and triggering dynamics whose evolution is probed and detected by the x-ray field [7–10]. One of the great achievements of

this new tool is the attosecond resolution obtained in real-time x-ray pump–probe spectroscopy measurement [6].

In this paper, we describe a conceptually different scheme of two-colour pump–probe spectroscopy: x-ray absorption by homonuclear diatomic molecules accompanied by core-hole hopping in the field of a strong IR laser. In contrast to the typical x-ray pump–probe scheme, the weak x-ray field here is used to create core holes in the lowest ungerade molecular orbital of the ground state by exciting the core electrons to the lowest unoccupied gerade molecular orbital, as determined by the dipole selection rules. Simultaneously with the core excitation, the IR radiation that is sufficiently strong to promote the ungerade core holes into the upper gerade core level mixes the two core-excited states of opposite parities and in that way changes the profile of the XA spectrum. The study of the XA spectrum modification by IR-induced core-hole hopping constitutes the main aim of our paper.

To exemplify the process studied, we have chosen a physical system in which the IR field with moderate intensity ($\gtrsim 10^{12}$ W cm⁻²) has time to promote the short-living core hole in another core level. Such a system is the homonuclear

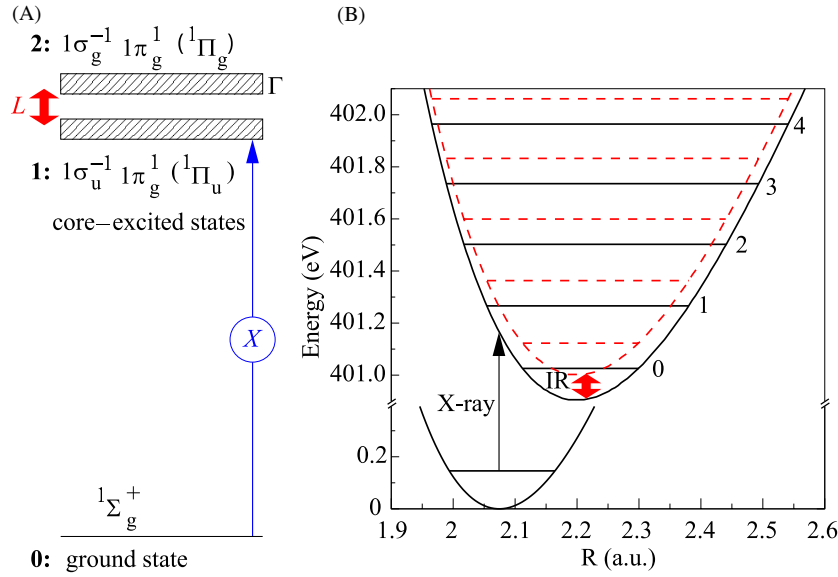


Figure 1. (A) Scheme of x-ray absorption accompanied by IR-induced transition between the ungerade and gerade core-excited states. (B) Potential energy curves of the ground state and the two close-lying core-excited states: $|1\sigma_u^{-1}1\pi_g^1\rangle$ (solid), $|1\sigma_g^{-1}1\pi_g^1\rangle$ (dashed).

diatomic molecule N_2 with a large dipole moment of the charge-transfer (CT) transition [11] between the core holes of opposite parities. We explore here the XA spectrum of the nitrogen molecule near the $1\sigma_u \rightarrow 1\pi_g$ resonance. It is worthwhile noting that the IR-laser-induced population of the symmetry forbidden core-excited state opens symmetry forbidden scattering channels and modifies the resonant inelastic x-ray scattering (RIXS) spectrum of the nitrogen molecule as well [12, 13].

The paper is organized as follows. The basic theory of XA accompanied by IR-induced core-hole hopping is presented in section 2.1. To give an insight into the physics of XA in the strong laser field, we solve the problem analytically for rectangular x-ray and laser pulses in section 2.2. The XA cross section of fixed-in-space molecules is shown in section 2.3. The orientation averaging for randomly oriented molecules is performed in section 2.4. The numerical simulations are discussed in section 3. Our findings are summarized in section 4.

2. Theory

2.1. X-ray absorption accompanied by core-hole hopping

In this section we present the general theory of interaction of a homonuclear diatomic molecule with strong low-frequency radiation (L) and weak high-frequency x-ray radiation (X):

$$\mathcal{E}_\alpha(t) = \mathbf{e}_\alpha E_\alpha(t) \cos(\omega_\alpha t + \varphi_\alpha), \quad \alpha = L, X. \quad (1)$$

Here \mathbf{e}_α , $E_\alpha(t)$ and ω_α are respectively the polarization vector, the amplitude and the frequency of the fields; φ_α is the phase of the fields and is assumed to be zero. We use the SI system of units. The theory is illustrated with the process of core-hole hopping in the nitrogen molecule. Thus, it is convenient to define the notation used in the general equations directly in terms of the electronic states of N_2 .

The ground-state (GS) electronic configuration of the N_2 molecule is

$$(1\sigma_g)^2, (1\sigma_u)^2, (2\sigma_g)^2, (2\sigma_u)^2, (1\pi_u)^4, (3\sigma_g)^2, \quad X^1\Sigma_g^+.$$

The lowest unoccupied molecular orbital in N_2 is the $1\pi_g$ orbital followed by two Rydberg orbitals: $3s\sigma_g$ and $3p\pi_u$. Here it is assumed that the frequency of the x-ray radiation is tuned near the strongest XA resonance $1\sigma_u \rightarrow 1\pi_g$. The weak x-ray field excites the molecule from the gerade GS $\equiv |0\rangle$ to the ungerade core-excited state $|1\sigma_u^{-1}1\pi_g^1\rangle \equiv |1\rangle$, while the strong laser (IR) field resonantly populates the close-lying upper gerade core-excited state $|1\sigma_g^{-1}1\pi_g^1\rangle \equiv |2\rangle$. The crucial point here is that the direct XA transition to $|2\rangle$ is forbidden by the dipole selection rules, whereas, as we will see below, the laser-induced CT transition $1\sigma_u \rightarrow 1\sigma_g$ is very strong. The scheme of the transitions is shown in figure 1(A).

It is worth noting that the strong laser field, in principle, is able to promote the $1\pi_g$ electron to any of the diffusive Rydberg states when the laser frequency is tuned in resonance with this transition ($\hbar\omega_L > 1$ eV). In this case one can expect significant Stark and ponderomotive shifts of the energy of the core-excited state [14, 15].

The symmetry allowed XA band $1\sigma_u \rightarrow 1\pi_g$ has an extensive vibrational structure, since the potential energy curves of the ground $|0\rangle$ and the core-excited $|1\rangle$ states are shifted with respect to each other (figure 1(B)). In contrast, it is not difficult to see that the potential energy curves of the close-lying core-excited states $|1\rangle$ and $|2\rangle$ are almost parallel to each other. These potential energy curves are taken as strictly parallel in the numerical simulations. Apparently, the IR-induced transition between the two core-excited parallel potentials occurs without a change of the vibrational state ν because

$$\langle 1, \nu | 2, \nu' \rangle = \delta_{\nu', \nu}. \quad (2)$$

In these terms the simultaneous interaction of the molecule with the radiation fields (1) is equivalent to x-ray-induced

mixing of the GS $|0, 0\rangle$ and the vibrational core-excited states $|1, \nu\rangle$ on one hand, and IR-induced mixing of the core-excited states $|1, \nu\rangle$ and $|2, \nu\rangle$ on the other hand. In other words, the external fields create an electron-nuclear wave packet $\psi = a_{0,0}|0, 0\rangle + \sum_{\nu}(a_{1,\nu}|1, \nu\rangle + a_{2,\nu}|2, \nu\rangle)$, where $a_{0,0} \approx 1$ can be assumed because the weak x-ray radiation almost does not alter the GS population. Let us denote the frequencies and the dipole-moment magnitudes of the transitions $|0, 0\rangle \rightarrow |1, \nu\rangle$ and $|1, \nu\rangle \rightarrow |2, \nu\rangle$ as $\omega_{1,\nu;0,0}$, d_{10} and ω_{21} , d_{21} , respectively, and assume that the lifetime broadening of the core-excited states, which is defined as half-width at half-maximum (HWHM), is the same ($\Gamma \equiv \Gamma_1 = \Gamma_2$). By applying the rotating wave approximation (RWA) to the weak x-ray field, but not to the strong laser radiation, we can describe the dynamics of the excited-state populations with the well-known amplitude equations

$$\begin{aligned} \dot{a}_{1,\nu} + \Gamma a_{1,\nu} &= \frac{i}{2} e^{i(\omega_{1,\nu;0,0} - \omega_X)t} G_{1,\nu;0,0}^X (\mathbf{e}_X \cdot \hat{\mathbf{d}}_\pi) \\ &+ i e^{-i\omega_{21}t} G_{21}^L \cos(\omega_L t) a_{2,\nu}, \\ \dot{a}_{2,\nu} + \Gamma a_{2,\nu} &= i e^{i\omega_{21}t} \cos(\omega_L t) G_{21}^L a_{1,\nu}, \quad G_{2,\nu;0,0}^X = 0. \end{aligned} \quad (3)$$

Here we introduce the Rabi frequencies of the x-ray and the laser fields

$$G_{1,\nu;0,0}^X = \frac{E_X(t) d_{10} \langle 1, \nu | 0, 0 \rangle}{\hbar}, \quad G_{21}^L = \frac{E_L(t) d_{21}}{\hbar} \cos \theta, \quad (4)$$

and denote with $\hat{\mathbf{d}}_\pi$ the unit vector along the direction of the transition dipole moment. Evidently, the Rabi frequency $G_{1,\nu;0,0}^X$ of the x-ray transition is different for each final vibrational state because of the different Franck–Condon (FC) amplitudes $\langle 1, \nu | 0, 0 \rangle$. The Rabi frequency G_{21}^L of the laser-induced transition $|1\rangle \rightarrow |2\rangle$ depends on the angle $\theta = \angle \mathbf{e}_L, \mathbf{R}$ between the polarization vector of the laser field and the vector of the internuclear distance.

The linearity with respect to the x-ray field allows us to extract the orientation factor $(\mathbf{e}_X \cdot \hat{\mathbf{d}}_\pi)$ in the amplitude equations (3) by replacing

$$a_{n,\nu} \rightarrow (\mathbf{e}_X \cdot \hat{\mathbf{d}}_\pi) a_{n,\nu}, \quad n = 1, 2. \quad (5)$$

The new amplitudes $a_{1,\nu}$ and $a_{2,\nu}$ obey the same equations as (3) except that the orientation factor can be eliminated as

$$(\mathbf{e}_X \cdot \hat{\mathbf{d}}_\pi) \rightarrow 1. \quad (6)$$

Thus, the amplitude equations (3) depend now only on the angle θ through the Rabi frequency G_{21}^L of the laser-induced transition.

Let us now show that strong population transfer from the symmetry allowed core-excited state $|1\rangle$ to the symmetry forbidden core-excited state $|2\rangle$ is possible within the short lifetime $1/\Gamma$ for moderate laser intensities I_L . The laser field leads to comparable populations of the two core-excited states ($|1\rangle$ and $|2\rangle$), see figure 1(A) when the time of the Rabi flopping $1/G_{21}^L$ is faster than the lifetime of the core-excited states $1/\Gamma$. This is fulfilled when the intensity of the laser field exceeds the threshold value

$$I_L > I_c, \quad I_c = 2c\epsilon_0 \left(\frac{\hbar\Gamma}{d_{21}} \right)^2. \quad (7)$$

We pay attention to the large dipole moment d_{21} of the CT transition [11] between the ungerade $|1\rangle$ and the gerade $|2\rangle$ core-excited states

$$\begin{aligned} \mathbf{d}_{21} &\equiv e \langle 1\sigma_u | \mathbf{r} | 1\sigma_g \rangle = \frac{e}{2} \int \mathbf{r} [1s^2(\mathbf{r} - \mathbf{R}_1) - 1s^2(\mathbf{r} - \mathbf{R}_2)] d\mathbf{r} \\ &\approx \frac{e}{2} [\mathbf{R}_1 - \mathbf{R}_2] = \frac{e\mathbf{R}}{2}. \end{aligned} \quad (8)$$

Here \mathbf{R}_1 and \mathbf{R}_2 are the radius vectors of the individual atoms and e is the electron charge. Inserting the value thus obtained $d_{21} = |\mathbf{d}_{21}| = eR/2 \approx 2.6379 D$ in (7), we get a reasonable value for the threshold intensity $I_c \sim 10^{12} \text{ W cm}^{-2}$.

2.2. X-ray absorption in the field of rectangular IR pulse

To get an insight into the dynamics of the excited-state populations, it is instructive to write the solution of (3) for fully overlapping rectangular x-ray and laser pulses. Here, we define the detuning of the x-ray and the laser fields relative to the resonant frequencies as $\Omega_{X,\nu} = \omega_X - \omega_{1,\nu;0,0}$ and $\Omega_L = \omega_L - \omega_{21}$, respectively. For simplicity, let us consider only one vibrational level of the core-excited states, i.e. $\Omega_{X,\nu} \rightarrow \Omega_X$. One can get an analytical solution by using the RWA for both fields:

$$\begin{aligned} \begin{pmatrix} \dot{a}_1 \\ \dot{a}_2 \end{pmatrix} &= \frac{iG_X e^{-i\Omega_X t}}{4\Delta} \begin{pmatrix} \Omega_L + \Delta \\ -G_{21}^L e^{-i\Omega_L t} \end{pmatrix} \\ &\begin{pmatrix} 1 - e^{-\Gamma t} e^{i(\Omega_X + \Omega_L/2 - \Delta/2)t} \\ \Gamma - i(\Omega_X + \Omega_L/2 - \Delta/2) \end{pmatrix} \\ &+ \begin{pmatrix} \Delta - \Omega_L \\ G_{21}^L e^{-i\Omega_L t} \end{pmatrix} \begin{pmatrix} 1 - e^{-\Gamma t} e^{i(\Omega_X + \Omega_L/2 + \Delta/2)t} \\ \Gamma - i(\Omega_X + \Omega_L/2 + \Delta/2) \end{pmatrix} \Bigg\}, \\ &0 \leq t \leq \tau, \end{aligned} \quad (9)$$

where τ is the duration of the strictly overlapping rectangular x-ray and laser pulses. We see that the XA resonance experiences Rabi splitting

$$\Delta = \sqrt{(G_{21}^L)^2 + \Omega_L^2}, \quad (10)$$

caused by the laser-induced transitions between the core-excited states.

When the detuning of both the x-ray and the laser field is zero ($\Omega_L = \Omega_X = 0$), the ratio of the excited-state populations ($\rho_n = |a_n|^2$) in the steady-state limit ($\Gamma t \gg 1$) is

$$\frac{\rho_2}{\rho_1} = \left(\frac{G_{12}^L/2}{\Gamma} \right)^2 = \frac{I_L}{I_c}. \quad (11)$$

When the intensity of the laser field I_L exceeds the threshold value I_c , more than 50% of the population of the ungerade core-excited state $|1\rangle$ is promoted to the gerade core-excited state $|2\rangle$. It is noteworthy that the laser-induced population of state $|2\rangle$ depends resonantly on the frequency of the laser field $\rho_2 \propto (G_{21}^L)^2 / [(\omega_L - \omega_{21})^2 + (G_{21}^L)^2]$, where the Rabi frequency results in a field broadening.

2.3. X-ray absorption cross section of fixed-in-space molecules

Firstly, let us consider x-ray absorption of molecules having defined orientation. In practice, such kind of measurements are

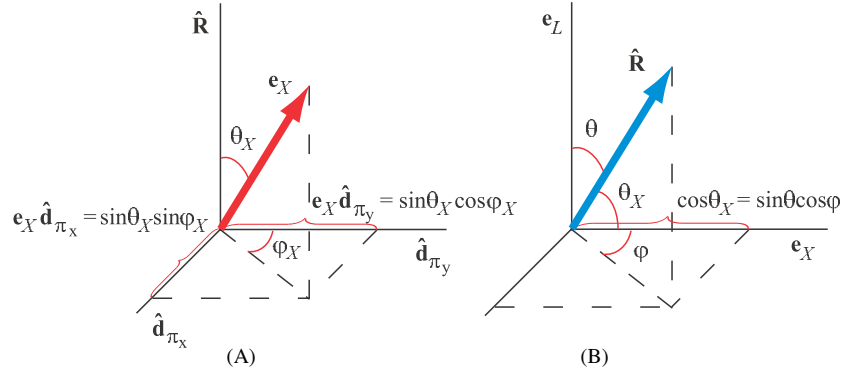


Figure 2. (A) Angles between the polarization vector \mathbf{e}_X of the incident x-ray pulse and the direction of the transition dipole moments $\hat{\mathbf{d}}_\pi$ of the core excitation $1\sigma_u \rightarrow 1\pi_g$ in the molecular frame. (B) Angle between the polarization vector \mathbf{e}_X of the x-ray pulse and the molecular axis \mathbf{R} in the laboratory frame when $\mathbf{e}_L \perp \mathbf{e}_X$.

performed through detecting the fragments of the dissociation caused by XA [1, 2] (see figure 3). The XA spectrum of fixed-in-space molecules is given by the population of the first core-excited state $|1\rangle$ which can be computed using equation (3). We only have to take into account the double degeneracy of this state ($1\sigma_u^{-1}1\pi_g^{(x)}$ and $1\sigma_u^{-1}1\pi_g^{(y)}$). The transition dipole moments of the core excitation into these two states are equal $|\mathbf{d}_{\pi_x}| = |\mathbf{d}_{\pi_y}| \equiv d_{10}$. Thus, replacement (5) results in the following expression for the populations of the core-excited states $\rho_{n,v}(\theta, \theta_X, t) = [(\mathbf{e}_X \cdot \hat{\mathbf{d}}_{\pi_x})^2 + (\mathbf{e}_X \cdot \hat{\mathbf{d}}_{\pi_y})^2] |a_{n,v}|^2$, where $\theta_X = \angle \mathbf{e}_X, \mathbf{R}$ is the angle between the polarization vector of the x-ray field and the molecular axis (see figure 2(A)). Finally, the populations of the core-excited states of fixed-in-space molecules are factorized into a product of two functions:

$$\begin{aligned} \rho_{n,v}(\theta, \theta_X, t) &= \sin^2 \theta_X \rho_{n,v}(\theta, \pi/2, t); \\ \rho_{n,v}(\theta, \pi/2, t) &= |a_{n,v}|^2, \quad n = 1, 2, \end{aligned} \quad (12)$$

which show explicitly the dependence on the angles θ_X and θ . These populations approach maximum when the molecular axis is perpendicular to the polarization vector of the x-ray field, $\mathbf{R} \perp \mathbf{e}_X$ ($\theta_X = \pi/2$).

Since the time of XA measurement is much longer than the lifetime of the core-excited states, the XA probability has to be integrated over time. The XA probability is given by the time integral of the populations of the symmetry allowed core-excited states times the lifetime broadening Γ . Therefore, the XA cross section of fixed-in-space molecules is

$$\begin{aligned} \sigma(\theta, \theta_X) &= \sin^2 \theta_X \sigma(\theta, \pi/2); \\ \sigma(\theta, \pi/2) &= \zeta \int_{-\infty}^{\infty} \sum_v \rho_{1,v}(\theta, \pi/2, t) dt, \end{aligned} \quad (13)$$

where the prefactor ζ contains all unessential for our investigation constants as well as the inverse flux of incident x-ray photons. We compute below the XA cross section of fixed-in-space molecules (13) in two cases: ($\theta_X = \pi/2, \theta = \pi/2$) and ($\theta_X = \pi/2, \theta = 0$), shown in figure 3.

2.4. Orientation averaging of the x-ray absorption cross section

Quite often x-ray absorption is measured for randomly oriented molecules. In this case, the XA cross section (13) has to be

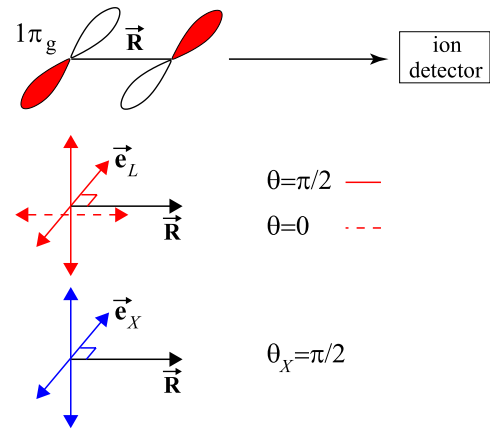


Figure 3. Scheme of x-ray absorption of fixed-in-space molecules [2].

averaged over all molecular orientations with respect to the polarization vectors \mathbf{e}_L and \mathbf{e}_X

$$\sigma = \frac{1}{2} \int_0^\pi \overline{\sin^2 \theta_X} \sigma(\theta, \pi/2) \sin \theta d\theta. \quad (14)$$

Here

$$\overline{\sin^2 \theta_X} = \frac{2}{3} [1 - P_2(\mathbf{e}_L \cdot \mathbf{e}_X) P_2(\cos \theta)] \quad (15)$$

is the expectation value of $\sin^2 \theta_X$ under rotation of the molecular axis around \mathbf{e}_L with fixed angle θ (figure 2(B)), and $P_2(x)$ is the Legendre polynomial. We investigate below two distinct geometries of the x-ray and IR fields: parallel ($\mathbf{e}_X \parallel \mathbf{e}_L$) and perpendicular ($\mathbf{e}_X \perp \mathbf{e}_L$) ones with

$$\overline{\sin^2 \theta_X} \rightarrow \begin{cases} \sin^2 \theta, & \parallel, (\mathbf{e}_X \parallel \mathbf{e}_L) \\ 1 - \frac{1}{2} \sin^2 \theta, & \perp, (\mathbf{e}_X \perp \mathbf{e}_L). \end{cases} \quad (16)$$

In fact, our assumption about the random orientation of the ground-state molecules is not valid in the general case, because the strong IR field aligns the rotationally cold molecules along the laser polarization vector [18]. This occurs also for the N_2 molecule due to anisotropy of its molecular polarizability. The IR-induced alignment of N_2 in the ground state has the order of magnitude [19] 10% for $T = 50$ K and $I_L = 2.5 \times 10^{12} \text{ W cm}^{-2}$. At first sight it seems that the resonant alignment of core-excited molecules can also be considerable. However, the IR field has no time to align the excited molecules due to

Table 1. Spectroscopic parameters of the core-excited states of N₂.

Core-excited state	$\hbar\omega_{c0}$ (eV) [exp.]	d_{c0}	$\hbar\Gamma$ (eV) [17]
$^1\Pi_u 1\sigma_u^{-1}1\pi_g^1\rangle$	400.88 [16]	1	0.0575
$^1\Pi_g 1\sigma_g^{-1}1\pi_g^1\rangle$	400.977 [16, 17]	0	0.0575
IR transition	$\hbar\omega_{21}$ (eV) [exp.]	d_{21} [theory]	–
$1\sigma_u^{-1}1\pi_g^1 \rightarrow 1\sigma_g^{-1}1\pi_u^1$	0.097 [17]	2.6379 Debye	–

Table 2. Relative Franck–Condon factors

$P_\nu = \langle 1, \nu|0, 0\rangle^2 / \langle 1, 0|0, 0\rangle^2$ and transition energies for the symmetry allowed $1\sigma_u \rightarrow 1\pi_g$ x-ray absorption vibronic transitions computed for Morse potential parameters from [20].

Vibronic state ν	$\hbar\omega_{1,\nu;0,0}$ (eV)	FC factor P_ν
0	400.88	1
1	401.12	0.927
2	401.36	0.500
3	401.59	0.208
4	401.82	0.0742
5	402.04	0.0242

their short lifetime ($1/\Gamma = 11.4$ fs) in comparison with the time of the laser-induced alignment ($\sqrt{T_{\text{rot}}/|G_{12}^L|} > 0.1$ ps). Here $T_{\text{rot}} = \hbar/2B$ and B is the rotational constant.

3. Numerical simulations

We solve numerically the amplitude equations (3) for each vibrational level of the core-excited electronic states after extracting the orientation factor (5) from the amplitudes. The RWA in (3) is used only to deal with the weak x-ray pulse, while the strong IR-laser pulse is treated strictly. We call the results so-obtained non-RWA (NRWA) solutions, in order to distinguish from the case in which both the x-ray and the IR fields are treated within the RWA. The populations of the core-excited states and the XA cross sections of fixed-in-space molecules are then calculated with formulae (12) and (13). For randomly oriented molecules the orientation averaging is performed with the help of (14) and (16) for both \parallel and \perp geometry. The incident x-ray and IR-laser pulses are assumed to have Gaussian temporal shapes,

$$E_\alpha(t) = E_\alpha^{(0)} \exp(-[(t - t_0)/\tau_\alpha]^2 \ln 2/2), \quad \alpha = X, L, \quad (17)$$

where τ_α is the width (HWHM) of the intensity profile, and t_0 is the peak position of the pulse. In the following numerical simulations, we tune the frequency of the IR field in exact resonance, $\Omega_L \equiv \omega_L - \omega_{21} = 0$.

The spectroscopic parameters of the core-excited states used in the calculations are collected in table 1. The excitation energy from the GS to the lowest ($\nu = 0$) vibrational level of the first core-excited state $^1\Pi_u$ is 400.88 eV [16], and the splitting between the molecular orbitals $1\sigma_g - 1\sigma_u$ is 0.097 eV [17]. In fact, the cited value is the spacing between the core-ionized $|1\sigma_u^{-1}\rangle$ and $|1\sigma_g^{-1}\rangle$ states. The splitting between the studied core-excited states $|1\sigma_u^{-1}1\pi_g^1\rangle$ and $|1\sigma_g^{-1}1\pi_u^1\rangle$ of the neutral N₂ molecule can be slightly different. The transition

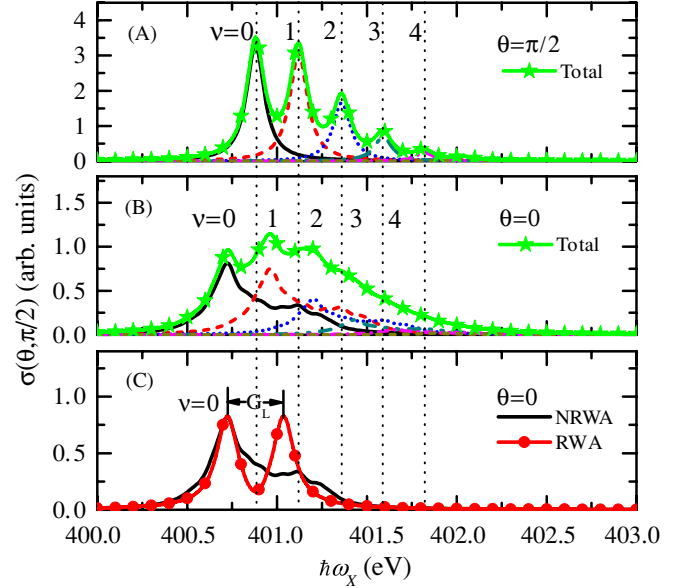


Figure 4. X-ray absorption spectrum $\sigma(\theta, \pi/2)$ of fixed-in-space N₂ molecules; $\theta = \angle \mathbf{e}_L, \mathbf{R}$, $\mathbf{e}_X \perp \mathbf{R}$, $I_L = 5 \times 10^{12}$ W cm⁻², $\tau_X = \tau_L = 50$ fs, $t_0 = 500$ fs, $\Omega_L = 0$. (A) and (B) show the strict NRWA solutions obtained with (3). The total XA profile is marked by stars, while the solid, dashed, dotted, etc lines display the partial XA cross sections. (C) Comparison of the RWA and the strict NRWA solutions of the partial XA cross sections ($\nu = 0$).

dipole moment d_{21} between the ungerade and gerade core-excited states is estimated at the equilibrium N₂ geometry ($R = 1.09768$ Å). The transition dipole moment d_{10} to the ungerade core-excited state $^1\Pi_u$ is normalized to unity and the transition dipole moment d_{20} to the gerade core-excited state $^1\Pi_g$ is zero owing to the dipole selection rules. The relaxation rate Γ is set to be 0.0575 eV (HWHM) [17]. Making use of the Morse potential parameters [20], we computed the relative FC factors and the transition energies to the symmetry allowed XA electron-vibrational transitions $1\sigma_u \rightarrow 1\pi_g$ with a time-dependent wave-packet code [21] (table 2). It is worth recalling that the potential curves of the two core-excited states are assumed to be parallel to each other.

The vibronic XA spectrum of fixed-in-space molecule is shown in figure 4. The polarization direction of the x-ray pulse is fixed to be perpendicular to the molecular axis, $\mathbf{e}_X \perp \mathbf{R}$, since then the absorption of x-ray photons is maximal (12). When the polarization vector of the laser pulse is also perpendicular to the molecular axis, $\theta = \angle \mathbf{e}_L, \mathbf{R} = \pi/2$, the Rabi frequency of the laser-induced transition G_{21}^L is zero (4). In this case, the IR-laser pulse does not induce any core-hole hopping between the ungerade and the gerade core-excited states and the conventional XA spectrum is obtained

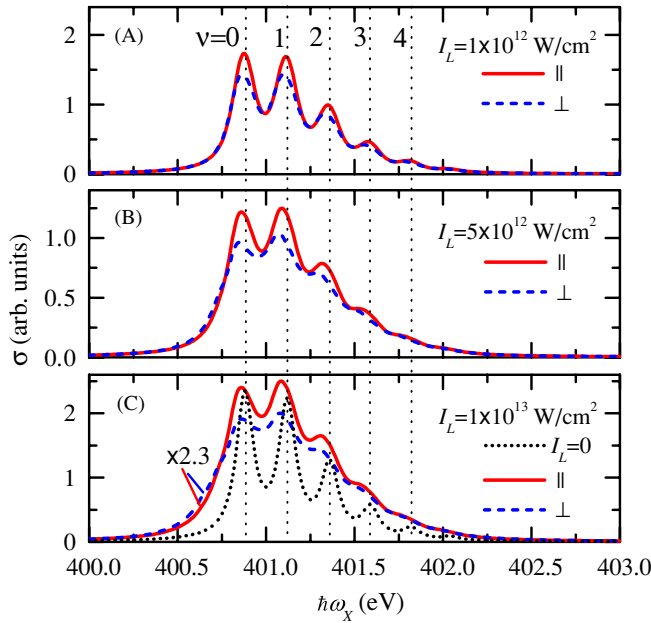


Figure 5. X-ray absorption spectrum σ of randomly oriented N_2 molecules for two geometries: \parallel ($\mathbf{e}_x \parallel \mathbf{e}_L$)—solid line and \perp ($\mathbf{e}_x \perp \mathbf{e}_L$)—dashed line; $\tau_x = \tau_L = 50$ fs, $t_0 = 500$ fs, $\Omega_L = 0$. (A)–(C) show the XA spectrum modification for different intensities of the laser field: $I_L = 1 \times 10^{12}$, 5×10^{12} and 1×10^{13} W cm^{-2} , respectively. The solid and dashed curves in (C) are enlarged 2.3 times, and the dotted line marks the conventional XA spectrum without the IR-laser field.

(figure 4(A)). However, when $\theta = 0$, one can see from figure 4(B) that the spectrum profile of XA is broadened and the resonant frequencies of all vibrational levels are shifted. The field broadening results in decrease of the x-ray absorption as one can see comparing figures 4(B) and (A). This is caused by the Rabi splitting (see also equation (10)).

Apparently, the RWA approximation for strong IR field is too crude when the Rabi splitting exceeds the IR frequency $G_{21} > \omega_L$. This we see clearly from figure 4(C) where the RWA and NRWA solutions are compared for the partial XA cross section ($\nu = 0$). One can see that the RWA solution fails to reproduce the asymmetry of the strict (NRWA) x-ray absorption profile because of $\hbar G_{21}^{L(0)} \approx 0.34$ eV $\gg \hbar \omega_{21}$ for $I_L^{(0)} = 5 \times 10^{12}$ W cm^{-2} .

The XA spectra of randomly oriented molecules for different intensities of the incident IR-laser pulse are shown in figure 5. One can see the broadening of the spectra and the shift of the resonances comparing with the conventional XA spectrum obtained without the IR field (dotted line in figure 5(C)). The effect becomes more pronounced (figure 5) with the increase of the IR-field intensity due to the enlargement of the Rabi splitting (10). However, in comparison with the XA spectrum of fixed-in-space molecules (figure 4(B)), the broadening and shift effects on the XA spectrum of randomly oriented molecules are softened. This owes to the orientation factor $\cos \theta$ in (4) which decreases the Rabi frequency of the IR transition G_{21}^L . Apparently, the anisotropy of the Stark broadening is exactly opposite

for the core excitation in the σ^* unoccupied molecular orbital in comparison with the $1\sigma_u \rightarrow 1\pi_g$ excitation. This means that the discussed effect gives direct information about the symmetry of the involved unoccupied molecular orbital. The IR-induced change of parity of the core hole opens symmetry forbidden channels of RIXS [12, 13]. The Stark broadening of XA resonances results in nonlinear dependence of the RIXS spectrum on the IR intensity [12, 13].

Let us comment briefly on the possibilities for experimental observation of the modifications of the XA spectrum caused by laser-induced hopping of core holes. In fact, such kind of measurement can be conducted with various symmetric molecules such as N_2 , O_2 or C_2H_2 . The main requirement is that the intensity of the IR pulse must be strong enough to make the time of the Rabi flopping of core holes comparable with the lifetime of the core-excited states. The estimations showed that a far-IR laser with a peak intensity $I_L \approx 10^{12}$ W cm^{-2} is sufficient for N_2 (7). Other molecules (O_2 and C_2H_2) need approximately the same intensity due to similar values of the CT transition dipole moments and the lifetime of the core holes. The effects discussed can be observed in a rather wide range of pulse durations (~ 100 ps–1 fs). One can expect phase sensitivity of the x-ray absorption when the IR pulse is short enough [13] ($\tau < 10$ fs). In principle, one can use a continuum-wave laser as well. An appropriate laser system would be the terawatt-power (TW) CO_2 laser [22]. The Accelerator Test Facility at Brookhaven National Laboratory is constructing a tabletop TW picosecond CO_2 laser system which will be synchronized with the electron bunches [23] and will provide a tool for observation of the XA spectrum modification caused by the Rabi flopping.

4. Summary

In this paper, we investigated theoretically a new two-colour pump–probe scheme of x-ray absorption accompanied by a strong IR-laser field. The laser field induces hopping of the core holes between the excited states of opposite parities, and changes the profile of the x-ray absorption spectrum. The effect of the IR-laser field on the x-ray absorption spectrum was studied in detail for the N_2 molecule. By applying the rotating wave approximation to the weak x-ray field and treating the strong IR field strictly, we solved the amplitude equations for each vibrational level of the core-excited states and got the vibronic x-ray absorption spectra for both fixed-in-space and randomly oriented molecules. It was found that the total profile of the vibronic x-ray absorption spectra is broadened and the resonances are shifted because of the Rabi splitting of the core-excited states caused by the strong IR pulse. The Rabi broadening leads to decrease of x-ray absorption. The rotating wave approximation for strong IR field fails to reproduce the asymmetry of x-ray absorption profile. The Stark broadening of the x-ray absorption spectrum depends on the orientation of the molecule and the angle between the polarization vectors of the x-ray and IR fields. The x-ray absorption of fixed-in-space molecules is a proper tool to detect the laser-induced core-hole hopping by an appropriate choice of the orientation of the IR polarization vector relative to the molecular axis.

The broadening and the spectral shifts of the XA spectrum are weakened for randomly oriented molecules in comparison with the fixed-in-space molecules because the Rabi frequency is different for different molecular orientations.

Acknowledgments

We acknowledge support from the Swedish Research Council (VR), Carl Tryggers Stiftelse (CTS) Foundation, and National Basic Research Program for China grant no. 2006CB806000.

References

- [1] Stöhr J 1992 *NEXAFS Spectroscopy* (Berlin: Springer)
- [2] Yagishita A, Shigemasa E and Kosugi N 1994 *Phys. Rev. Lett.* **72** 3961
- [3] Bressler C and Chergui M 2004 *Chem. Rev.* **104** 1781
- [4] Techert S, Schotte F and Wulff M 2001 *Phys. Rev. Lett.* **86** 2030
- [5] Neutze R, Wouts R, Techert S, Davidsson J, Kocsis M, Kirrander A, Schotte F and Wulff M 2001 *Phys. Rev. Lett.* **87** 195508
- [6] Drescher M, Hentschel M, Klenberger R, Ulberacker M, Yakovlev V, Scrinzi A, Westerwalbesloh Th, Kleineberg U, Heinzmann U and Krausz F 2002 *Nature* **419** 803
- [7] Cubaynes D *et al* 2004 *Phys. Rev. Lett.* **92** 233002
- [8] Schulz J *et al* 2006 *Phys. Rev. A* **74** 012705
- [9] Felicissimo V C, Guimarães F F and Gel'mukhanov F 2005 *Phys. Rev. A* **72** 023414
- [10] Felicissimo V C, Guimarães F F, Gel'mukhanov F, Cesar A and Ågren H 2005 *J. Chem. Phys.* **122** 094319
- [11] Mulliken R S 1939 *J. Chem. Phys.* **7** 14
- [12] Liu J-C, Velkov Y, Rinkevicius Z and Gel'mukhanov F 2008 *Chem. Phys. Lett.* **453** 117
- [13] Liu J-C, Velkov Y, Rinkevicius Z and Gel'mukhanov F 2008 *Phys. Rev. A* **77** 043405
- [14] Buth C, Santra R and Young L 2007 *Phys. Rev. Lett.* **98** 253001
- [15] Mulser P, Uryupin S, Sauerbrey R and Wellegenhasen B 1993 *Phys. Rev. A* **48** 4547
- [16] Glans P, Skytt P, Gunnelin K, Guo J-H and Nordgren J 1996 *J. Electron. Spectrosc. Relat. Phenom.* **82** 193
- [17] Liu X-J, Prümper G, Gel'mukhanov F, Cherepkov N A, Tanaka H and Ueda K 2007 *J. Electron. Spectrosc. Relat. Phenom.* **156–158** 73
- [18] Peterson E R *et al* 2008 *Appl. Phys. Lett.* **92** 094106
- [19] Torres R, de Nalda R and Marangos J P 2006 *Phys. Rev. A* **72** 023420
- [20] Feifel R *et al* 2002 *Phys. Rev. Lett.* **89** 103002
- [21] Salek P 2003 *Comput. Phys. Commun.* **150** 85
- [22] Tochitsky S Ya, Narang R, Filip C, Clayton C E, Marsh K A and Joshi C 1999 *Opt. Lett.* **24** 1717
- [23] Yakimenko V 2007 *Tabletop TW picosecond CO₂ Laser Project* http://www.bnl.gov/atf/core_capabilities/co2sys.asp (accessed 25 March 2008)